



## Strathprints Institutional Repository

Mirantsev, Leonid V. and Sonnet, Andre and Virga, Epitanio G. (2012) *Geodesic defect anchoring on nematic shells*. Physical Review E, 86 (2). ISSN 1539-3755

Strathprints is designed to allow users to access the research output of the University of Strathclyde. Copyright © and Moral Rights for the papers on this site are retained by the individual authors and/or other copyright owners. You may not engage in further distribution of the material for any profitmaking activities or any commercial gain. You may freely distribute both the url (<http://strathprints.strath.ac.uk/>) and the content of this paper for research or study, educational, or not-for-profit purposes without prior permission or charge.

Any correspondence concerning this service should be sent to Strathprints administrator: <mailto:strathprints@strath.ac.uk>

## Geodesic defect anchoring on nematic shells

Leonid V. Mirantsev

*Institute of the Problems of Mechanical Engineering, Academy of Sciences of Russia, St. Petersburg 199178, Russia*

André M. Sonnet

*Department of Mathematics and Statistics, University of Strathclyde, Livingstone Tower, 26 Richmond Street, Glasgow G1 1XH, Scotland*

Epifanio G. Virga

*Dipartimento di Matematica Università di Pavia, Via Ferrata 1, 27100 Pavia, Italy*

(Received 15 January 2012; revised manuscript received 23 June 2012; published 23 August 2012)

Nematic shells are colloidal particles coated with nematic liquid crystal molecules, which may freely glide and rotate on the colloid's surface while keeping their long axis on the local tangent plane. Molecular dynamics simulations on a nanoscopic spherical shell indicate that under appropriate adhesion conditions for the molecules on the equator, the equilibrium nematic texture exhibits at each pole a pair of  $+\frac{1}{2}$  defects so close to one another to be treated as one  $+1$  defect. Spirals connect the polar defects, though the continuum limit of the interaction potential would not feature any elastic anisotropy. A molecular averaging justifies an anchoring defect energy that feels the geodesics emanating from the defect. All our observations are explained by such a geodesic anchoring, which vanishes on flat manifolds.

DOI: [10.1103/PhysRevE.86.020703](https://doi.org/10.1103/PhysRevE.86.020703)

PACS number(s): 61.30.Jf

Nematic shells are thin films of nematic liquid crystal (LC) deposited on the boundary of colloidal particles whose size may go down to the nanoscopic range [1]. Here nematic molecules are envisaged as particles with a preferred direction  $\ell$  (called the *spin*, for short) that prefers to lie on the colloid's boundary  $\mathcal{S}$ . Molecules are thought of as freely gliding on  $\mathcal{S}$  with their spin freely rotating in the local tangent plane.

The nematic director  $\mathbf{n}$ , defined as an ensemble average of the molecular spin  $\ell$ , is thus a unit vector field everywhere tangent to  $\mathcal{S}$ , for which a theorem of Poincaré [2] requires the sum  $m$  of the topological charges of all defects to be the Euler characteristic of  $\mathcal{S}$ , which is a topological invariant. In particular, if  $\mathcal{S}$  has the same topology as a sphere,  $m = 2$ .

Since the proposal was made [3] that nematic shells could be employed as building blocks for the new chemistry of *metamaterials*, where atoms are replaced by colloids [4,5], there has been growing interest in defects on nematic shells, as they could act as *hot spots* capable of attracting polymeric ligands [6,7]. Thus, the number of defects on a nematic shell would become the *valence* of the colloid surrounded by the shell and so determine the whole metamaterial architecture. For example, spherical colloids are spontaneously tetravalent, with four  $+\frac{1}{2}$  defects, which may or may not be located at the vertices of an inscribed, regular tetrahedron [8–11]. Pictorially, they are effectively represented as tennis balls, whose seams evoke the shell's nematic texture [3]. Changes in the colloids' valence can be induced by either external fields or deformations [12–14].

In this Rapid Communication we consider spherical shells on which the nematic director is prescribed along an equator, so as to make molecules prefer to be oriented in the direction of the local meridian: We would expect that such a localized anchoring promotes a global alignment along meridians, with two  $+1$  defects, one at each pole, prevailing in the equilibrium texture. The shell would then resemble a divalent *spindle* instead of tetravalent tennis ball. However, the outcomes of a molecular dynamics (MD) simulation indicate that this is

not the case: While at each pole two  $+\frac{1}{2}$  defects are so close that they can effectively be treated as a single  $+1$  defect, the director arrangement around them is not rich in splay as in a spindle, but rather rich in bend as in a vortex. Thus, the equilibrium nematic texture spontaneously develops spirals, which, when merged in their opposite winding variants, host deeply metastable defects. A purely elastic model is unable to explain these findings, unless a bend-to-splay anisotropy is artificially introduced, which finds no justification in the molecular interaction potential. Based precisely on this potential, we rather find an extra anchoring energy at defects which depends on both the colloid's curvature and its geodesic field; this energy makes vortices preferred.

In our MD experiment, the nematic shell is a spherical crust of LC molecules free to glide and rotate in the interstice between two concentric, spherical solid layers consisting of fixed molecules, which provide an effective degenerate planar anchoring for the LC molecules. The interaction potential is  $V = V_{\text{iso}}(r_{12}) + V_{\text{aniso}}(r_{12}, \ell_1 \cdot \ell_2)$  [15], where  $r_{12}$  is the distance between the centers of mass of the interacting molecules and

$$V_{\text{iso}}(r_{12}) = 4\varepsilon_{\text{iso}} \left[ \left( \frac{\sigma}{r_{12}} \right)^{12} - \left( \frac{\sigma}{r_{12}} \right)^6 \right], \quad (1a)$$

$$V_{\text{aniso}}(r_{12}, \ell_1 \cdot \ell_2) = -\varepsilon_{\text{aniso}} \left[ \frac{3}{2} (\ell_1 \cdot \ell_2)^2 - \frac{1}{2} \right] \left( \frac{\sigma}{r_{12}} \right)^6. \quad (1b)$$

In Eqs. (1),  $\sigma$  is the characteristic range of the interaction (of the order of the molecular size) and  $\varepsilon_{\text{iso}}$  and  $\varepsilon_{\text{aniso}}$  are the isotropic and anisotropic interaction strengths, respectively. For  $\varepsilon_{\text{aniso}} > 0$ ,  $V_{\text{aniso}}$  favors the alignment of molecular spins in one and the same direction, whereas for  $\varepsilon_{\text{aniso}} < 0$ ,  $V_{\text{aniso}}$  favors the alignment of molecular spins at right angles to one another. We set  $\varepsilon_{\text{aniso}} = \varepsilon_{\text{iso}} > 0$ , for the interactions between LC molecules, and  $\varepsilon_{\text{aniso}} = -20\varepsilon_{\text{iso}} < 0$  (with one and the

same value of  $\varepsilon_{\text{iso}}$ ), for the interactions between fixed and mobile molecules.

The simulation crust (with 7284 molecules) has inner radius  $R = 18\sigma$  and thickness  $2\sigma$ , while the adjacent layers with fixed molecules (7954 inside and 14380 outside) have both thickness  $3\sigma$  (the usual MD cutoff length [16]). The centers of mass of the molecules fixed in the layers were frozen in random positions with their spins aligned in the radial direction. This makes LC molecules prefer to lie with their spins on the local tangent plane. The shell's volume was kept constant, as was the reduced temperature  $T^* = k_B T / \varepsilon_{\text{iso}} = 0.9$ , where  $T$  is the absolute temperature and  $k_B$  is the Boltzmann constant. The value prescribed for  $T^*$  is well below the nematic-to-isotropic transition temperature in bulk,  $T_{NI}^* = 1.05$ , obtained for a similar model system [17].

Simulations were started both from random distributions of molecules' centers of mass and spins, and from configurations where (only) spins were well ordered. All simulations were run for a number of time steps necessary to reach an equilibrium state of the system (one time step is equal to 0.001 in dimensionless MD units). At each time step, the equations of motion of classical particle dynamics were solved numerically by the method described in ([16], § 3.2.1) (see Ref. [17] for details), and the temperature of the system was kept constant by appropriately rescaling both translational and rotational velocities of the particles. To describe the local orientational order, we introduced polar coordinates  $(\theta, \phi)$  on the sphere of radius  $R$ , with  $\theta$  being the colatitude and  $\phi$  the longitude. At any given point  $(\theta_0, \phi_0)$  with surface normal  $\mathbf{v}_0$ , we computed averages  $\langle \cdots \rangle_{\mathcal{C}}$  over a probing spherical cap  $\mathcal{C}$  with prescribed aperture,<sup>1</sup>

$$\mathbf{Q} := \langle \boldsymbol{\ell} \otimes \boldsymbol{\ell} - \frac{1}{2} \mathbf{P}(\mathbf{v}) \rangle_{\mathcal{C}}, \quad (2)$$

where  $\mathbf{P}(\mathbf{v}) = \mathbf{I} - \mathbf{v} \otimes \mathbf{v}$  is the projector over the local tangent plane ( $\mathbf{I}$  is the identity in space and  $\mathbf{v}$  is the unit normal). The largest eigenvalue  $\lambda$  of  $\mathbf{Q}$  is the local *scalar order parameter* and the corresponding eigenvector  $\mathbf{n}$  of  $\mathbf{Q}$  defines the *average director*, which we write as  $\mathbf{n} = \cos \beta \mathbf{v} + \sin \beta \cos \alpha \mathbf{e}_\theta + \sin \beta \sin \alpha \mathbf{e}_\phi$  in the frame  $(\mathbf{e}_\theta, \mathbf{e}_\phi, \mathbf{v})$ , where  $\mathbf{e}_\theta$  is along the local meridian and  $\mathbf{e}_\phi = \mathbf{v} \times \mathbf{e}_\theta$  is along the local parallel. Along the equator ( $\theta = \frac{\pi}{2}$ ), molecules were fixed with their spin parallel to the local meridian ( $\alpha = 0, \beta = \frac{\pi}{2}$ ).<sup>2</sup>

The continuum limit of the interaction potential  $V$  can be obtained as follows. Suppose that in a *regular* molecular spin texture, that is, away from defects, a molecule sits at the point  $p$  with orientation  $\boldsymbol{\ell}$ . We imagine that the first neighbor molecules in its vicinity are distributed in equilibrium along a geodesic

circle of radius  $r$ .<sup>3</sup> For  $r \ll R$ , we can represent the points  $p_u$  on this circle as  $p_u = p + r\mathbf{u}$ , with  $\mathbf{u}$  varying in the unit circle  $\mathbb{S}^1$  on the tangent plane to  $p$ . Correspondingly, in the absence of defects, the spin  $\boldsymbol{\ell}_u$  at  $p_u$  can be expressed as

$$\boldsymbol{\ell}_u = \boldsymbol{\ell} + r(\nabla_s \boldsymbol{\ell})\mathbf{u} + \frac{1}{2}r^2(\nabla_s^2 \boldsymbol{\ell}) \cdot (\mathbf{u} \otimes \mathbf{u}) + o(r^2), \quad (3)$$

where  $\nabla_s$  denotes the surface gradient. Replacing in Eqs. (1)  $r_{12}$  with the fixed equilibrium radius  $r$ , to within an inessential additive constant, we can write the elastic energy density  $W_e$  of a regular texture as  $W_e = -\frac{3}{2}\rho\varepsilon_{\text{anisotropy}}\langle (\boldsymbol{\ell} \cdot \boldsymbol{\ell}_u)^2 \rangle_{\mathbb{S}^1}$ , where  $\rho$  is the *surface* number density and  $\langle \cdots \rangle_{\mathbb{S}^1}$  is the average over  $\mathbf{u} \in \mathbb{S}^1$ . Since at the molecular scale  $\boldsymbol{\ell}$  can be viewed as a tangential unit vector field [so that  $(\nabla_s \boldsymbol{\ell})^\top \boldsymbol{\ell} = \mathbf{0}$ ] and  $\langle \mathbf{u} \otimes \mathbf{u} \rangle_{\mathbb{S}^1} = \frac{1}{2}(\mathbf{I} - \mathbf{v} \otimes \mathbf{v})$ , it follows from Eq. (3) that<sup>4</sup>

$$W_e = \frac{K}{2} |\nabla_s \boldsymbol{\ell}|^2 \quad \text{with} \quad K = \frac{3}{2}\rho\varepsilon_{\text{anisotropy}}r^2. \quad (4)$$

Thus, in a continuum, purely elastic model, where the nematic shell is identified with an ideal spherical surface  $\mathcal{S}$  of radius  $R$  and  $\boldsymbol{\ell}$  is replaced by  $\mathbf{n}$ , the free-energy functional reads as  $\mathcal{F}_e[\mathbf{n}] := \frac{K}{2} \int_{\mathcal{S}} |\nabla_s \mathbf{n}|^2 da$ , where  $K$  is a phenomenological modulus and  $a$  denotes the area measure. Letting  $\alpha = \alpha(\theta, \phi)$  be the angle that  $\mathbf{n}$  makes with the local meridian  $\mathbf{e}_\theta$ , we set  $\mathcal{F}_e = \frac{K}{2} F_e$ , where

$$F_e[\alpha] = \int_0^\pi \left[ \sin \theta \int_0^{2\pi} \left( \alpha_{,\theta}^2 + \frac{\alpha_{,\phi}^2 + 1}{\sin^2 \theta} \right) d\phi \right] d\theta, \quad (5)$$

subject to the adhesion condition  $\alpha(\frac{\pi}{2}, \phi) = 0$ . As also known from the study of nematic defects in the plane ([19], § 4.2.2), the functional (5) attains no minimum, but once a small *core* region is carved away from either pole ( $\theta = 0, \pi$ ), it is minimized by  $\alpha \equiv 0$ . The corresponding molecular configuration is a *spindle* exhibiting a +1 defect at each pole. As convincing as the elastic model may seem, this conclusion was *not* confirmed by our MD experiment.

We started a MD simulation from a random initial configuration, and in equilibrium we arrived at a spiralling configuration with two  $+\frac{1}{2}$  defects at each pole so close to one another to be viewed as a single +1 defect, and with extra, deeply metastable  $\pm\frac{1}{2}$  dipoles [20]. Figure 1 illustrates the corresponding equilibrium molecular alignment seen from above the north pole, which features a *vortex*. We attempted to annihilate artificially the defects in each dipole by randomizing the molecules' orientation in a path of cells joining them and then letting the dynamics evolve again: We succeeded in erasing all dipoles but two, one above the equator and the other below it, thus arriving at the configuration represented in Fig. 2 by a Mercator map of the average director. We repeated the simulation, starting from the spindle configuration

<sup>1</sup>To ensure that the number and distribution of the molecules entering the average are independent of the actual position of the point on the sphere, we included all molecules that lie within a cone with axis  $\mathbf{v}_0$ , apex in the center of the sphere, and aperture  $2\gamma$ , where  $\gamma$  is a fixed angle. We used  $\gamma = 6^\circ$ . Explicitly, the criterion for including in the average a molecule situated at  $(\theta, \phi)$  with surface normal  $\mathbf{v}$  is  $\mathbf{v}_0 \cdot \mathbf{v} > \cos \gamma$ .

<sup>2</sup>We also performed MD simulations with all molecules completely free. As expected, the configurations attained at equilibrium had four  $+\frac{1}{2}$  defects.

<sup>3</sup>The geodesic circle of radius  $r$  and center  $p$  on a surface  $\mathcal{S}$  is the locus of points at the distance  $r$  on all geodesics of  $\mathcal{S}$  issued from  $p$ , each tangent at  $p$  to precisely one unit vector  $\mathbf{u} \in \mathbb{S}^1$  (see, for example, Ref. [18], p. 177). For a sphere, the geodesics at one point are the great circles through that point and the geodesic circles are the latitude lines having that point as pole.

<sup>4</sup>Letting  $\ell_{i,j}$  denote the local Cartesian components of  $\nabla_s \boldsymbol{\ell}$ , to obtain Eq. (4), we also made use of the identity  $\ell_i \ell_{i,jj} = -\ell_{i,j} \ell_{i,j}$ .



FIG. 1. Equilibrium vortex at the north pole.

(with the molecules' centers of mass randomly distributed in the spherical crust). At equilibrium, we obtained again a configuration qualitatively similar to that depicted in Fig. 2.

The two dipoles shown in Fig. 2 and their metastability suggest that the shell's ground state is spiralling around two vortices: Such a state, actually existing in two equivalent variants (with opposite windings), gives rise to metastable blends, where defect dipoles are topologically necessary. To confirm this suggestion, we performed a MD simulation starting from a pure spiralling ordered state, which at equilibrium delivered a dipole-free molecular arrangement preserving the original winding (with still one vortex at each pole). This clearly contradicts the elastic model based on the free-energy functional  $\mathcal{F}_e$ , unless we split  $|\nabla_s \mathbf{n}|^2$  into  $(\text{div}_s \mathbf{n})^2 + |\mathbf{n} \times \text{curl}_s \mathbf{n}|^2$  and attribute artificially a larger elastic weight to the surface splay energy  $(\text{div}_s \mathbf{n})^2$  than to the surface bend energy

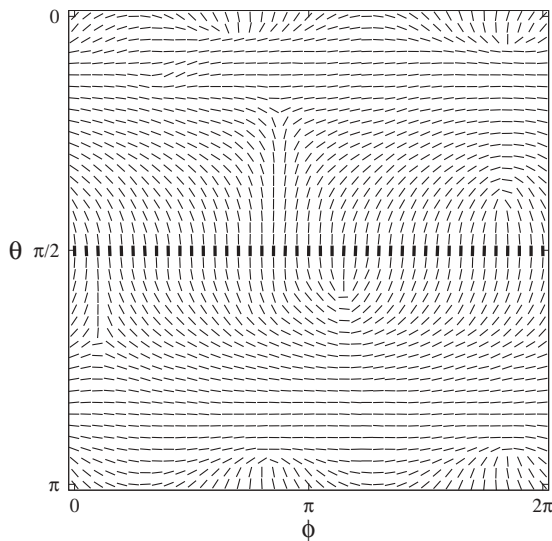


FIG. 2. Mercator map of  $\mathbf{n}$  in the  $(\phi, \theta)$  plane. For all directors  $\beta \approx \frac{\pi}{2}$ . Those frozen along the equator (for which  $\beta = \frac{\pi}{2}$ ) are thicker than the others.

$|\mathbf{n} \times \text{curl}_s \mathbf{n}|^2$ .<sup>5</sup> To explain our observations, we take here a different avenue, which extends the continuum limit (4) to defect textures.

Consider now a molecule with orientation  $\ell$  sitting in the core  $p_0$  of a defect. We imagine it surrounded at equilibrium by the first neighbor molecules distributed along a geodesic circle of radius  $r_c$  around  $p_0$ . In polar coordinates  $(\theta, \phi)$  with pole at  $p_0$ , the equation of this circle is  $\theta = \theta_c := r_c/R$  and the geodesics emanating from  $p_0$  have unit tangent  $\mathbf{u}$  represented by  $\mathbf{u} = \cos \phi \ell + \sin \phi \ell_\perp$ , where  $\ell_\perp := \mathbf{v} \times \ell$ . Correspondingly, the molecular orientation  $\ell_u$  on the geodesic circle can be written as  $\ell_u = \cos \alpha \mathbf{e}_\theta + \sin \alpha \mathbf{e}_\phi$ , where  $\alpha = \alpha(\phi)$ . For a defect with topological charge  $m$ ,  $\alpha = \alpha_0 + (m-1)\phi$ . In particular, for  $m = 1$ ,  $\alpha_0 = 0$  yields a radial surface *hedgehog*, where the average director flux lines are along geodesics, and  $\alpha_0 = \frac{\pi}{2}$  yields a *ring*, where the average director flux lines are orthogonal to geodesics; intermediate values of  $\alpha_0$  yield *vortices*. For  $m \neq 1$ , the phase  $\alpha_0$  does not alter the shape of the average director flux lines; it only makes them rotate about  $p_0$ . A simple computation shows that  $\ell \cdot \ell_u = \cos \alpha \cos \theta_c \cos \phi - \sin \alpha \sin \phi$ . When  $m = 1$ , extending the continuum limit for a regular director texture, we give the energy  $W_c = -\frac{3}{2} \varepsilon_{\text{aniso}} \langle (\ell \cdot \ell_u)^2 \rangle_{\mathbb{S}^1}$ , here associated with a defect core, the following form (to within an additive constant):

$$W_c = \frac{K_c}{2} \sin^2 \theta_c \cos^2 \alpha_0 = \frac{K_c}{2} \frac{r_c^2}{R^2} \cos^2 \alpha_0 + o\left(\frac{r_c^2}{R^2}\right), \quad (6)$$

with  $K_c = \frac{3}{2} \varepsilon_{\text{aniso}}$ . This energy, concentrated at every  $+1$  defect, supplements the diffused elastic energy  $\mathcal{F}_e$ . Since  $W_c$  is minimized by  $\alpha_0 = \frac{\pi}{2}$ , the total texture energy  $\mathcal{F} = \mathcal{F}_e + W_c$  is unlikely to be minimized by a spindled director arrangement, which would require  $\alpha_0 = 0$ .  $W_c$  is more than a mere core energy: it is a defect anchoring energy that makes the average director prefer the orientation *at right angles* with the geodesics emanating from a  $+1$  defect.<sup>6</sup> Thus, if  $m = 1$ , vortices prevail over radial hedgehogs as do spirals over spindles. For  $m \neq 1$ , a similar computation yields  $W_c = \frac{K_c}{4} \frac{r_c^2}{R^2} + o\left(\frac{r_c^2}{R^2}\right)$ , independent of the phase  $\alpha_0$ . In particular, for  $m = \frac{1}{2}$ , which is the case for spherical shells with no prescribed ordering on the equator, each defect contributes one and the same energy and the underlying geodesics play no role in defect anchoring. Finally, since  $W_c$  vanishes in the limit as  $R \rightarrow \infty$ , a geodesic anchoring only acts on defects in curved shells.

Letting  $\alpha(\theta)$  be the angle that the average director  $\mathbf{n}$  makes with  $\mathbf{e}_\theta$  and writing  $\mathcal{F}_e$  as in Eq. (5) and  $W_c$  as in Eq. (6), with  $K_c$  a phenomenological modulus, by neglecting an additive constant we can set  $\mathcal{F} = 2\pi K F[\alpha]$  with

$$F[\alpha] = \int_{\theta_c}^{\frac{\pi}{2}} \alpha_{,\theta}^2 \sin \theta d\theta + \frac{1}{\nu} \cos^2 \alpha_c, \quad (7)$$

<sup>5</sup>Here  $\text{div}_s$  and  $\text{curl}_s$  denote the surface divergence and the surface curl, respectively. A surface vortex has virtually no splay energy, whereas a surface radial hedgehog has virtually no bend energy.

<sup>6</sup>To emphasize that the favorable orientation is *not* along geodesics, but at right angles with them, one could well call this anchoring *antigeodetic*.

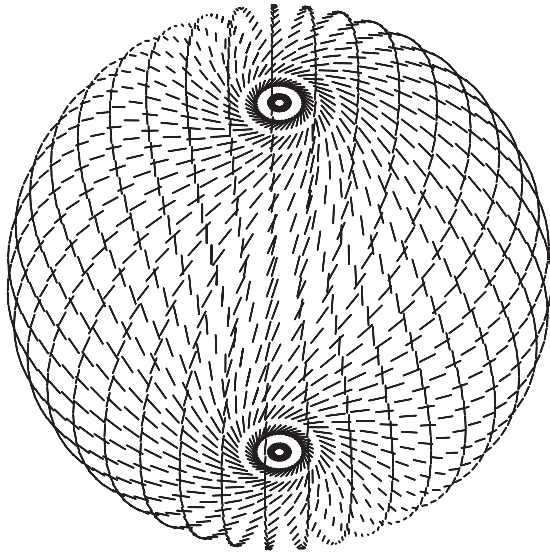


FIG. 3. Loxodromes for  $\nu = \frac{1}{2}$ ,  $\theta_c = 1/50$ , and  $\alpha_c \doteq 0.45\pi$ .

where  $\theta_c = r_c/R$ ,  $\alpha_c := \alpha(\theta_c)$ , and  $\nu := 2\pi K R^2 / K_c r_c^2$ . The solutions to the Euler-Lagrange equation for  $F$  are the equilibrium loxodromes  $\alpha_*(\theta) = c[\ln(1 - \cos \theta) - \ln(\sin \theta)]$ , where, for  $r_c \ll R$ ,  $c \simeq -\alpha_c \ln(2R/r_c)$ . By evaluating  $F[\alpha_*]$  we obtain a function of  $\alpha_c$ ; its minimizer is  $\alpha_c = 0$  for  $\nu > \ln(2R/r_c)$ , and it varies in the interval  $]0, \frac{\pi}{2}[$  for  $\nu < \ln(2R/r_c)$ , converging to  $\frac{\pi}{2}$  as  $\nu \rightarrow 0$ . For  $\alpha_c = 0$ ,  $\alpha_*$  represents a spindle, whereas it represents spirals for  $0 < \alpha_c < \frac{\pi}{2}$ . For  $\nu = \frac{1}{2}$  and  $\theta_c = 1/50$ , the average director field corresponding to  $\alpha_*$  is illustrated in Fig. 3.

According to Eq. (7), if at the equator molecules were required to be orthogonal to meridians ( $\alpha(\frac{\pi}{2}) = \frac{\pi}{2}$ ),  $F$  would attain its minimum for  $\alpha \equiv \frac{\pi}{2}$ , irrespective of both  $\theta_c$  and  $\nu$ . We performed a MD simulation with this constraint, starting from a random initial condition; indeed we found at equilibrium a pure-bend molecular arrangement with rings (not vortices) at the poles.

In conclusion, MD simulations in a spherical crust mimicking a nematic shell revealed features that a simple elastic model, justified in the continuum limit of the molecular interaction potential, was unable to explain. When the same continuum limit is applied to the core of a +1 defect, an extra anchoring energy emerges, which would orient the average director at right angles with the geodesics emanating from the defect. Such a concentrated energy would by itself induce vortices wherever a +1 defect is formed by either topological or elastic frustration. We also showed by a phenomenological model that the interplay between elastic energy and geodesic anchoring is subtle and the latter does not always prevail.

Geodesic defect anchoring is characteristic of curved shells; it vanishes on flat surfaces. Moreover, for what our study of a spherical shell could reveal, it does not seem to be relevant to defects of topological charge  $m \neq 1$ . For a general surface, we expect it to depend nontrivially on the quadratic invariants of the curvature tensor. There, it could also play a role for defects with  $m \neq 1$ , in deciding where they are more likely to be located at equilibrium.

We thank the Reviewers for their valuable remarks on a previous version of the manuscript. Financial support from GNFM (a branch of INdAM, the Italian National Institute for Higher Mathematics) is gratefully acknowledged.

- 
- [1] T. Lopez-Leon and A. Fernández-Nieves, *Colloid Polym. Sci.* **289**, 345 (2011).
  - [2] H. Poincaré, *J. Math. Pures Appl.* **2**, 151 (1886).
  - [3] D. R. Nelson, *Nano Lett.* **2**, 1125 (2002).
  - [4] G. A. DeVries, M. Brunnbauer, Y. Hu, A. M. Jackson, B. Long, B. T. Neltner, O. Uzun, B. H. Wunsch, and F. Stellacci, *Science* **315**, 358 (2007).
  - [5] S. C. Glotzer and M. J. Solomon, *Nat. Mater.* **6**, 557 (2007).
  - [6] E. C. Nelson and P. V. Braun, *Science* **318**, 924 (2007).
  - [7] Zhang, A. S. Keys, T. Chen, and S. C. Glotzer, *Langmuir* **21**, 11547 (2005).
  - [8] M. A. Bates, *J. Chem. Phys.* **128**, 104707 (2008).
  - [9] H. Shin, M. J. Bowick, and X. Xing, *Phys. Rev. Lett.* **101**, 037802 (2008).
  - [10] T. Lopez-Leon, A. Fernández-Nieves, M. Nobili, and C. Blanc, *Phys. Rev. Lett.* **106**, 247802 (2011).
  - [11] T. Lopez-Leon, V. Koning, K. B. S. Devaiah, V. Vitelli, and A. Fernández-Nieves, *Nat. Phys.* **7**, 391 (2011).
  - [12] G. Skačej and C. Zannoni, *Phys. Rev. Lett.* **100**, 197802 (2008).
  - [13] S. Kralj, R. Rosso, and E. G. Virga, *Soft Matter* **7**, 670 (2011).
  - [14] M. A. Bates, G. Skačej, and C. Zannoni, *Soft Matter* **6**, 655 (2010).
  - [15] G. R. Luckhurst and S. Romano, *Proc. R. Soc. London A* **373**, 111 (1980).
  - [16] M. Allen and D. J. Tildesley, *Computer Simulations of Liquids* (Clarendon Press, Oxford, 1987).
  - [17] M. Pereira, A. Canabarro, I. de Oliveira, M. Lyra, and L. Mirantsev, *Eur. Phys. J. E* **31**, 81 (2010).
  - [18] J. J. Stoker, *Differential Geometry*, Pure and Applied Mathematics, Vol. XX (Wiley, New York, 1969).
  - [19] P. G. de Gennes and J. Prost, *The Physics of Liquid Crystals*, 2nd ed. (Clarendon Press, Oxford, 1993).
  - [20] R. L. B. Selinger, A. Konya, A. Travesset, and J. V. Selinger, *J. Phys. Chem. B* **115**, 13989 (2011).